Geosynthetic overlap for reinforced piled embankment: centrifuge modelling

Luc Thorel[1], *Mathieu* Guerois[1], *Thierry* Dubreucq[1*], *Matthieu* Blanc[1]
[1] University Gustave Eiffel, Lab. Centrifuges for Geotechnics (GERS-CG), France

Abstract. The overlap of two geosynthetic strips, located at the base of the granular load transfer platform and above rigid inclusions, is being studied on small-scale instrumented models using the moving tray device in the geotechnical centrifuge at the University Gustave Eiffel. The width of the cover (in the range between zero and the pile spacing, for 3 area ratios of reinforced pile embankment) influences the efficiency of the load transfer and the differential settlement at the surface.

1 Introduction

The piled embankment on Rigid Inclusion (RI) is a type of reinforcement used in loose soils for geotechnical works. It is a composite foundation in which multiple phenomena are involved to transfer loads to the deep foundation via the Load Transfer Platform (LTP) and then to reduce differential settlement [1]. It has the advantage of being built without waiting for the compressible soil to 'finish' settling and of having a reduced environmental impact thanks to the savings in materials [2]. As part of the national ASIRI+ project (2019-2024), new research is being developed to improve understanding of this technique, and in particular on geosynthetic (GSY) reinforced LTP installed horizontally at the base of the LTP.

The question raised here concerns the overlap of adjacent GSYs, their width and their location. The investigation technique is based on the physical modelling of simplified, centrifuged small-scale models.

GSY-reinforced piled embankment is a technique used for the foundation of large-area constructions, such as road or rail structures, on loose soils. In addition to load transfer through an 'arching' effect [1], GSY reinforcement can develop a 'membrane' effect [6, 26], which increases the efficiency of load transfer to the RIs. If these RIs (with a pile cap of diameter a), are part of a square mesh (with spacing s), its area ratio, characterising the soil surface covered by the RIs is:

$$\alpha = \pi a^2 / 4s^2 \quad (1)$$

Such an embankment (Figure 1) is generally composed of a granular platform to transfer the load, RI's pile cap (optional) to homogenise and control α, and RI themselves, which reach the geological formation capable of taking up the load. In the field, a working platform is usually implemented, but this is not the subject of this study. To simplify the experiments,

* Corresponding author: thierry.dubreucq@univ-eiffel.fr

a single layer of granular material is used in the physical model. This corresponds to the LTP, but also to the backfill. The terminology 'rigid inclusion' is similar to 'disconnected pile', meaning that the deep foundation is not connected to the superstructure.

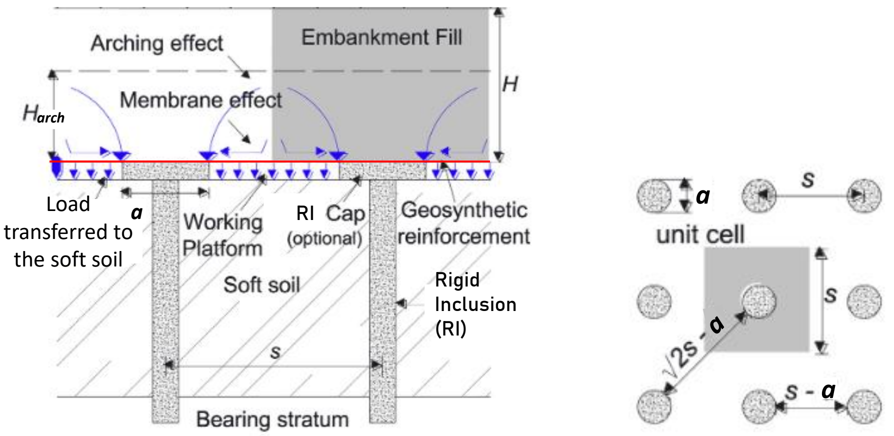

Fig.1. Elements of a piled embankment (adapted from [9]).

The load transfer efficiency E is used to assess the quality of the load transfer. It is the ratio, on a unit cell, of F the vertical load on the RI and the total load above, due to the weight of the entire embankment and any vertical surcharge force q [3] :

$$E = \frac{F}{\gamma H s^2 + q} \tag{2}$$

The design of an embankment (possibly reinforced with GSY) on RI follows national standards such as the ASIRI recommendations [3] in France, the EBGEO standards [11] in Germany, BS8006 [8] in the UK, or CUR226 in Netherlands [9, 27].

The main objective of this study is to observe and analyse the influence of GSY overlaps at the base of the LTP during a parametric experimental campaign conducted in a centrifuge. The height H of the LTP is constant. The width and position of the overlap were tested for 3 different spacings s, and compared with the case of a continuous GSY (Figure 2-0), but only the position of the overlap in line with an RI line (Figure 2-1) is detailed here for α = 1.23%.

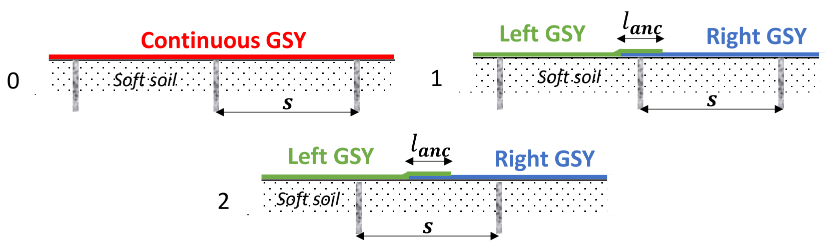

Fig.2. Geometrical configurations: (0) continuous GSY; (1) GSY overlap centered on a RI line; (2) GSY overlap between 2 RI lines.

GSY reinforcement [17, 20] is commonly used for RI embankments as it significantly increases the load transfer efficiency of the foundation [7, 17, 26]. Geogrids (GGR) allow soil to interlock within their mesh to create a rigid cover comparable to a reinforced slab [23].

They are generally placed at the bottom of the LTP, or inside the LTP [16]. Only the case of the GGR at the base of the LTP is studied here.

When unidirectional GSYs are used (reinforcement mainly in one direction), two layers of geosynthetics are required, one reinforced in each direction. In some cases, bi-directional GSYs are used with a single layer. A single stiffness of a 2D GSY is considered here (Table 1).

Geosynthetics are produced in the form of wound strips, the size of which depends on the manufacturer (a few metres wide, a few hundred metres long). Joints between strips are generally unavoidable, both in width and length. The minimum overlap between two adjacent strips is l_{anc}=0.3 m [3]. It is considered here as the main variable to be studied.

2 Centrifuge modelling

Approaches at various scales are useful to study the role of GSY reinforcement in embankments on RI: centrifuge modelling [10, 19, 22], 1×g models [24] or numerical analysis [2]. Only centrifugal modelling will be used here.

2.1 The geo-centrifuge of the University Gustave Eiffel

Operational since 1985, the centrifuge at the University Gustave Eiffel [25] has a radius of 5.5 m. At the end of the arm, a swinging basket carries a small-scale model, with a maximum load of 2 tonnes at 100×g.

The centrifuge modelling technique enables the same level of stress to be reproduced on the small-scale model as on the prototype (full-scale) model. Scale factors (Table 1) are used to design the centrifugal scale model to match the full-scale prototype [12].

Table 1. Scaling factors for the current centrifuge modelling

Dimension	*Unit*	*Prototype*		*N×g model*	
Length/height	*m*	*1*	*a = 0.3 / s = 2.4*	*1/N*	*a = 0.025 / s = 0.2*
Gravity	*m/s²*	*1*		*N*	
Force	*kN*	*1*		*1/N²*	
Mass	*kg*	*1*		*1/N³*	
Stress	*kPa*	*1*		*1*	
Strain	*%*	*1*		*1*	
Area ratio (α)	*%*	*1*		*1*	
Density	*kg/m³*	*1*		*1*	
Settlement (y)	*m*	*1*		*1/N*	
Efficiency (E)	*%*	*1*		*1*	
Tension (T)	*kN/m*	*1*	*long. 63 / transv. 57*	*1/N*	*756 / 684*
Stiffness (J)	*kN/m*	*1*	*840*	*1/N*	*10080*

2.2 Experimental device

The Mobile Tray Device (MTD), is installed in the centrifuge basket to simulate the settlement of loose soil (Figure 3): the perforated tray, on which the granular LTP is installed, moves downwards (thanks to 3 servo jacks), allowing the RIs to punch the LTP [7, 21].

The MTD has been used in the past to perform parametric studies on LTP, using the same sand (a mixture of dense Hostun sand fractions) as in the present study [5].
Blanc et al. [7] investigated the mechanisms in GSY-reinforced LTP at a gravity of 20×g and showed that prestressing has no significant impact on performance. It was also shown that

the differential surface settlements of the LTP were lower using GSY than without GSY, for the same applied stress.

Fagundes et al. [10] observed that differential surface settlement is more influenced by the distance between RIs or the thickness of the LTP than by the presence of a GSY. They also showed that surface settlement is zero for H/(s-d)>2.1, and possibly for smaller values if the spacing between RIs is smaller.

Blanc et al. [6] showed that the stiffer the GSY, the better the membrane effect.

Girout et al. [13] showed that charge transfer increases with α, but that decreasing the spacing of RIs is more effective than increasing *a*, the diameter of the RI. The arching effect also increases with the friction angle *φ'* of the LTP. The efficiency *E* increases with *H, a, φ'*, or the applied stress and decreases with *s*.

Girout et al. [14] also showed that if a total 'arching effect' is developed, the presence of GSY does not improve the load transfer. They also showed that the best load transfer is obtained for a GSY located at the base of the LTP.

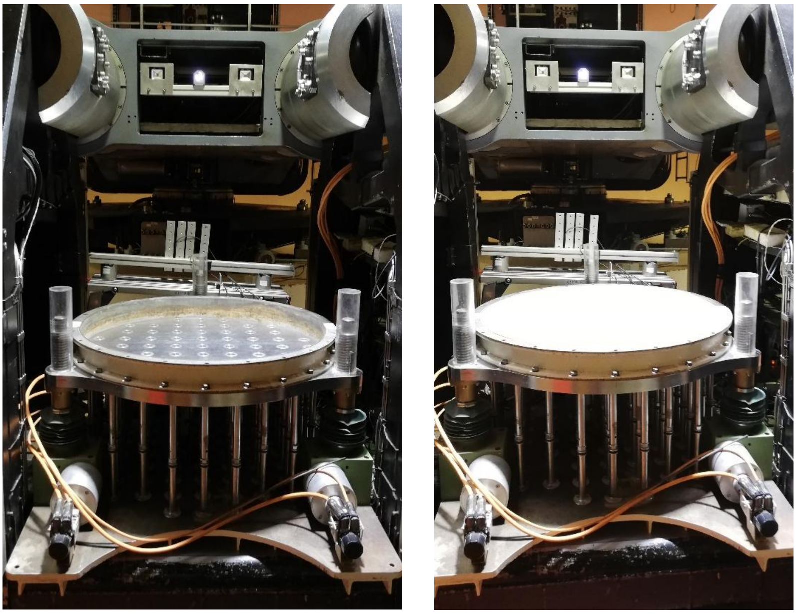

Fig. 3. The Mobile Tray Device in the centrifuge basket: empty (left) and filled with the granular LTP (right)

The MTD has shown interesting possibilities for studying the behaviour of granular LTP and interactions with a continuous GSY. In the current configuration, the area ratio, the backfill and the LTP are identical, consisting of a granular material, but the geometry of the GSY is the key parameter in this study.

2.3 Instrumentation

The instrumentation included the measurement of the force transmitted to the RI, the settlement of the top surface of the LTP and the load on the tray. It should be noted that the measurements were not the same for each campaign. The tests were instrumented with:

- 9 force transducers in the 9 central RIs, designed for axial measurement,

- 2 LASER displacement sensors, placed under the plate to measure displacement in its centre and peripheral position,
- 4 LASER settlement sensors on the surface of the LTP: above an RI y_{MP}, above the centre of a cell y_{MS}, between two adjacent RI y_{MS2},
- 2 force sensors inserted in the plate (if possible) measuring the load in the middle of a cell.

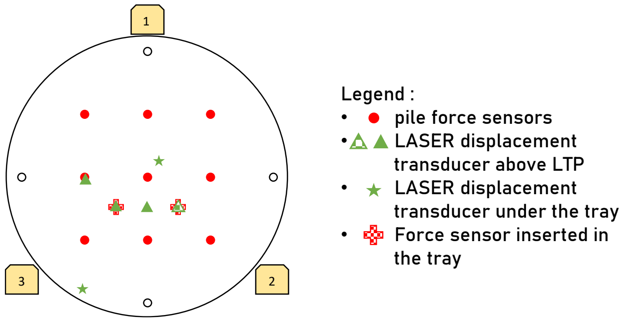

Fig.4. Top view of the sensors' location ($\boldsymbol{\alpha}$ = 1.23 %)

The data collected with the sensors on the model centrifuge is digitalized using a Quantum Digital Analogue Converter, then transferred by optical fibre to the storage computer. The data was recorded and displayed at 0.1 or 1 Hz (depending on the phase of testing) using CATMAN data acquisition software.

2.4 Typical result: overlapping over a line of Rigid Inclusions

For α=1.23%, it is possible to include a vertical load cell instead of an RI in a free hole diameter on the plate. Typical results [15] are shown in Figure 5 with different overlaps on the left and right sides of the middle RI row. The load transfer efficiency is shown in black on the left axis, the mesh centre stress on the tray in red dashed lines on the second left axis, and the settlement efficiency on either side of the overlap, $\Delta y_{\_MS}/s$, in green and blue on the right axis.

At the start of the test (phase I), the load measured on the MTD over an area $\pi.a^2/4$ increases, as does E, corresponding to a gradual tensioning of the GSY and perhaps a rearrangement of the force chains in the LTP. For a continuous GSY (Figure 5a), the maximum load on the plate corresponds to about half the weight of the LTP on top of the transducer. As there is little or no arching effect, all the load at the top of the GSY starts to be carried by the GSY and follows a possible triangular distribution. The maximum load on the plate is obtained for a displacement of 40 to 50% of the RI diameter.

In phase II, the tension in the GSY can be observed with a lower rate of increase in E and a reduction in the load on the plate (down to zero). When the GSY is no longer in contact with the plate (phase III), the charge on the plate is zero.

For any overlap configuration, as the strips are symmetrically aligned with the RI row (or between two rows), symmetrical behaviour is expected. This is true for differential settlement under a certain displacement of the tray (Figure 5, blue and green lines). The reduced differential settlement, in the middle of a mesh on the left and right sides of the overlap line, was measured: on the side with the lower face of the overlap (right side), the reduced differential settlement is higher than on the other side from a certain MTD settlement. For both tests, the maximum difference between the two sides was 0.5%.

The load analysis seems to follow the mechanics of continuous media in phase I and perhaps phase II, until the discontinuity generated by the 'cut' or overlap gradually plays a role and modifies the initial continuity of the whole structure. For example, Figure 5b shows a series of sudden efficiency losses, which are probably compensated for in other parts of the model (where no instrumentation is unfortunately available).

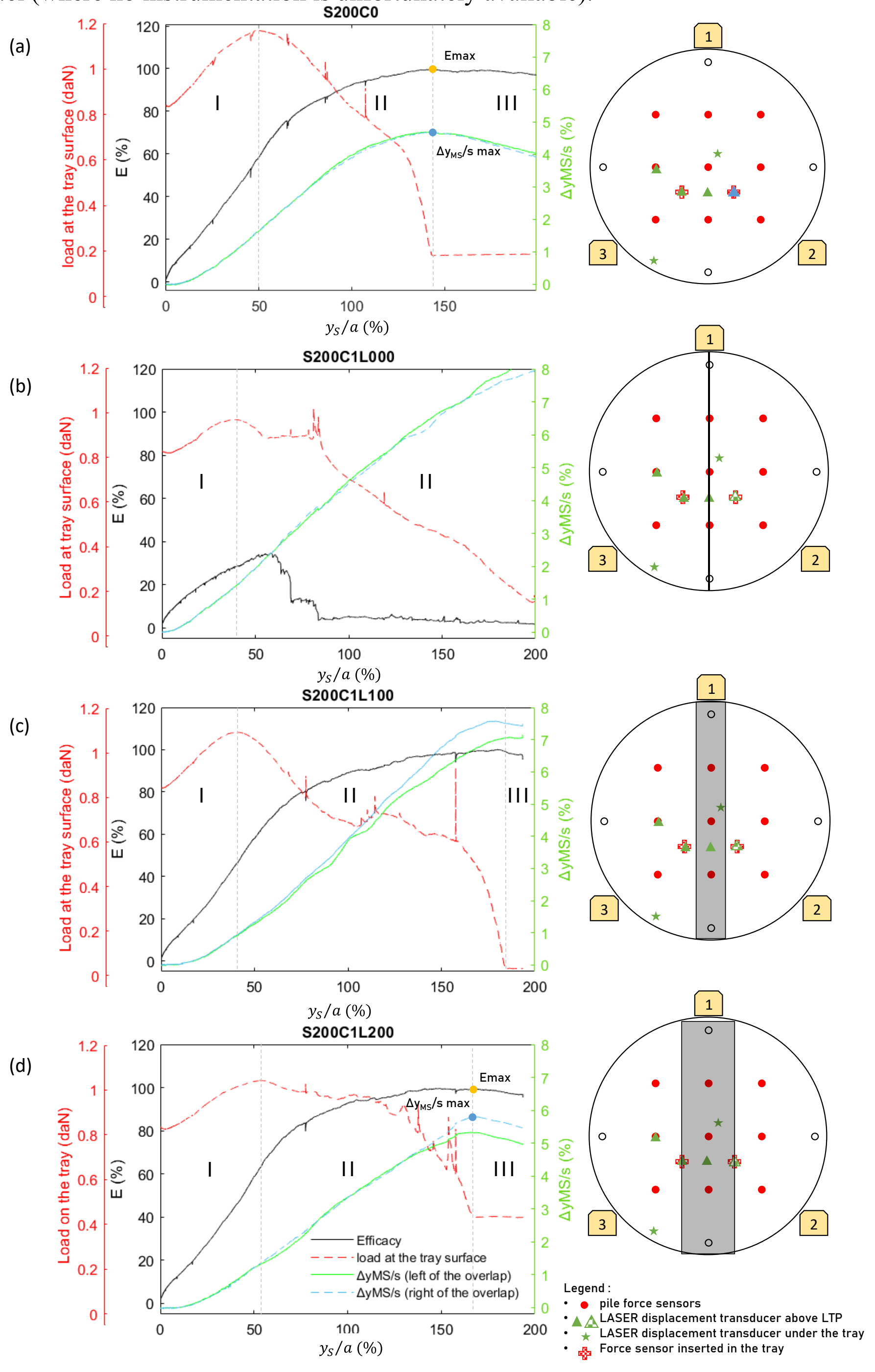

Fig. 5. Efficiency of the load transfer E, load in the centre of the mesh on the mobile tray and variation of the efficiency expressed in differential settlement $\Delta y_{MS}/s$ on each side of the overlap, versus the dimensionless settlement y_S/a of the MT for : (a) continuous GSY, (b)) $l_{anc} = 0$, (c) $l_{anc} = s/2$, (d) $l_{anc} = s$.

3 Conclusions

Experiments on centrifuged small-scale models have shown that increasing the overlap width improves load transfer efficiency and reduces differential settlement at the surface of the load transfer platform.

It was observed that the load transferred to the ‘soft ground’ (at the tray surface) increases at the beginning of the tray movement, due to the tensioning of the GSY or the rearrangement of the LTP. The efficiency corresponding to the maximum load (end of phase I) increases with the length of the overlap.

For small GSY overlaps, poor characteristics are observed (low efficiency and high differential settlement). However, as the overlap increases, the behaviour tends to be similar to that of the continuous geosynthetic test. For a cover greater than s/2, we observe a behaviour very close to that of the continuous GSY for settlements of less than one RI diameter. For higher compressible soil settlements, the differential settlement gradually diverges, while the effectiveness is little changed. This tends to show that the ‘critical’ overlap width is more sensitive to a differential settlement criterion than to an efficiency criterion.

Other configurations need to be studied: other values for the spacing between RIs, other overlap positions (not centred on a line of RIs), etc.

4 Acknowledgements

The authors would like to thank the ASIRI+ French National Programme for funding this research, and in particular Alain Nancey for supplying the geosynthetic, but also for very good advice. Special thanks to the technical centrifuge team of the University Gustave Eiffel which contributed to the development of the experiments, in particular Alexandre Jagu and Alain Néel.

References

1. M. Almeida de S.S., M.E.S. Marques, Design and Performance of Embankments on Very Soft Soils. CRC Press, London (2013)
2. M. Almeida de S.S., D.F. Fagundes, L. Thorel, M. Blanc, Geosynthetic-reinforced pile-embankments: numerical, analytical and centrifuge modelling. Geosynth. Int. **27**, 301–314. (2020) https://doi.org/10.1680/jgein.19.00011
3. ASIRI Recommendations for the design, construction and control of rigid inclusion ground improvements. ISBN9782859784706, Presses des Ponts, 383p (2013)
4. ASIRI+ Improvement and reinforcement of soils by rigid inclusions. (2019) https://asiriplus.fr/ (accessed on 27th nov. 2024)
5. G. Baudouin, F. Rosquoët, J. Canou, J.C. Dupla, L. Thorel, G. Rault, I. Andria-Ntoanina, Caractérisation mécanique d'un mélange de sables d'Hostun. Journées Nationales de Géotechnique et de Géologie de l’Ingénieur Nantes 18-19 juin JNGG08. ISBN 9782720825204. pp 491-498. (2008) https://www.geotech-fr.org/download.php?type=pdf&doc=jngg-2008
6. M. Blanc, L. Thorel, R. Girout, M. Almeida de S.S., Geosynthetic reinforcement of a granular load transfer platform above rigid inclusions: comparison between centrifuge testing and analytical modelling. Geosynthetics international. February 2014, Vol.**21**, 1, pp.37-52. (2014) DOI: 10.1680/gein.13.00033

7. M. Blanc, G. Rault, L. Thorel, M. Almeida de S.S., Centrifuge investigation of load transfer mechanisms in a granular mattress above a rigid inclusions network. Geotext. Geomembr. **36**, 92–105. (2013) https://doi.org/10.1016/j.geotexmem.2012.12.001
8. BS8006 Code of practice for strengthened/reinforced soils and other fills. BS8006-1. British Standard Institution. ISBN 978-0-580-53842-1 (2010)
9. CUR226. See van Eekelen and Brugman, 2016 (below).
10. D.F. Fagundes, M. Almeida de S.S., L. Thorel, M. Blanc, Load transfer mechanism and deformation of reinforced piled embankments. Geotext. Geomembr. **45**, 1–10. (2017) https://doi.org/10.1016/j.geotexmem.2016.11.002
11. EBGEO Recommendations for Design and Analysis of Earth Structures using Geosynthetic Reinforcements - EBGEO. John Wiley & Sons (2012)
12. J. Garnier, C. Gaudin, S.M. Springman, P.J. Culligan, D. Goodings, D. Konig, B. Kutter, R. Phillips, M.F. Randolph, L. Thorel, Catalogue of scaling laws and similitude questions in geotechnical centrifuge modelling. Int. J. Phys. Modelling in Geotechnics ISSN 1346-213X, **7**, n°3, pp 1-24. (2007) doi.org/10.1680/ijpmg.2007.070301
13. R. Girout, M. Blanc, L. Thorel, D.F. Fagundes, M. Almeida de S.S., Arching and deformation in a piled embankment: centrifuge tests compared to analytical calculations. Journal of Geotechnical and Geoenvironmental Engineering **142**(12), 10p (2016) https://doi.org/10.1061/(ASCE)GT.1943-5606.0001557
14. R. Girout, M. Blanc, L. Thorel, D. Dias, Geosynthetic reinforcement on piled-supported embankment Geosynthetics International. Vol.**25**, n°1 37–49. (2018) https://doi.org/10.1680/jgein.17.00032
15. M. Guerois, Centrifuge parametric study of the geosynthetic overlap above piled embankment foundations. Internship report University Gustave Eiffel/ Polytech'Clermont.122p (2023)
16. P. Gunnvard, H. Mattsson, J. Laue, Evaluating the Design Criteria for Light Embankment Piling: Timber Piles in Road and Railway Foundations. Appl. Sci. **12**, 166. (2022) https://doi.org/10.3390/app12010166
17. A. Nancey, L. Briançon, Lessons learned from the ASIRI+ project on the use of geosynthetics in load transfer platform, Eurogeo8, Lille (2025)
18. A. Huckert, Optimisation with numerical and experimental approaches of the mechanical properties of geosynthetic materials used in soil renforcement (in french) .Ph.D. Dissertation, Univ. Grenoble. (2014) https://www.theses.fr/2014GRENI030
19. L. King, A. Bouazza, C. Gaudin, C.D. O'Loughlin, H.H. Bui, Behavior of geosynthetic-reinforced piled embankments with defective piles. J. of Geotechnical and Geoenvironmental Engineering, **145**(11), 04019090. (2019)
20. M.F. Msouti, J.C. Blivet, D. Levacher, Comportement au fluage des géotextiles en renforcement mécanique. Laboratoire central des ponts et chaussées. 143p. (1997)
21. G. Rault, L. Thorel, A. Néel, S. Buttigieg, F. Derkx, G. Six, U. Okyay, Mobile tray for simulation of 3D load transfer in pile-supported earth platforms. 7th int. Conf. on Phys. Modelling in Geotechnics June 28th- july 1st, Zurich, Springman, Laue, Seward (eds) Taylor & Francis Group, London, ISBN 978-0-415-59288-8, pp.261-266 (2010)
22. P.Shen, C. Xu, J. Han, Centrifuge tests to investigate global performance of geosynthetic-reinforced pile-supported embankments with side slopes. Geotextiles and Geomembranes, **48**(1), 120-127 (2020)

23. B. Simon, L. Briançon, L. Thorel, Amélioration des sols par inclusions rigides : le rôle des géosynthétiques dans la plateforme de transfert de charge. Rev. Fr. Géotechnique 1. (2020) https://doi.org/10.1051/geotech/2020003
24. C. Terqueux, L. Briancon, P. Delmas, D. Jacqueline, J. Racinais, A. Pantet, P. Gotteland, Renforcement d'un sol compressible par inclusions rigides: étude des transferts de charge au sein de la plateforme granulaire renforcée par des géosynthétiques, in: 11èmes Journées Nationales de Géotechnique et de Géologie de l'ingénieur. (2022)
25. L. Thorel, Physical Modelling Facilities: from Galileo to 3D Printing. Presented at the ICPMG 2022, 10th International Conference on Physical Modelling in Geotechnics, Korean Geotechnical Society, Seoul, Korea, ISBN 978-89-952197-7-5, 64-72. (2022) https://www.issmge.org/uploads/publications/53/115/P00503.pdf
26. S.J.M. van Eekelen, A. Bezuijen, H.J. Lodder, A.F. van Tol, Model experiments on piled embankments. Part I. Elsevier Enhanced Reader. (2012) https://doi.org/10.1016/j.geotexmem.2011.11.002
27. van Eekelen, S.J.M., Brugman, M.H.A., 2016, Eds. Design Guideline Basal Reinforced Piled Embankments (called 'CUR226'). CRC press, Delft, Netherlands, ISBN 9789053676240, in English.